materials

MDPI

Article

Study on the Evolution Mechanism of Carbon Impurities in Polysilicon Production Based on HSC Simulation

Yu Hou [1,2,*], Xueqian Lv [2] and Guoqiang Huang [1,3,*]

[1] School of Chemical Engineering and Technology, Tianjin University, Tianjin 300350, China
[2] Xinjiang Xinte Crystalline Silicon High-Tech Co., Ltd., Urumqi 830011, China; lvxueqian@163.com
[3] State Key Laboratory of Chemical Engineering and Low-Carbon Technology, Tianjin University, Tianjin 300350, China
* Correspondence: houyu202512@163.com (Y.H.); hgq@tju.edu.cn (G.H.); Tel.: +86-185-9933-7722 (Y.H.)

Abstract

The existing forms and evolution mechanisms of carbon impurities constitute the core scientific issue in the optimization of polysilicon purification processes. The depth of research on this issue directly determines the targeting and effectiveness of directional impurity removal strategies, and is even a key prerequisite for improving the quality and reducing the cost of polysilicon products. Based on HSC simulation calculations and using the Gibbs free energy of reactions as the judgment criterion, this paper investigated the existing forms and evolution mechanism of carbon impurities during the production of polysilicon via the modified Siemens process. The results show that the evolution mechanism of carbon impurities is as follows: the solute carbon in silicon powder reacts with hydrogen to generate CH_4. Subsequently, CH_4 synergistically undergoes radical rearrangement and the Rochow reaction with methylchlorosilanes in chlorosilane and CH_4 in recovered hydrogen. Meanwhile, $CH_3\cdot$ radicals combine with radicals generated from chlorosilanes to form a mixture of methylchlorosilanes dominated by $SiH(CH_3)Cl_2$ as well as CH_4. After distillation purification, $SiH(CH_3)Cl_2$ enters the $SiHCl_3$ stream, and then synergistically undergoes cracking and radical rearrangement with CH_4 in high-purity hydrogen, the solid-soluble elemental carbon forms and deposits in polysilicon. Simultaneously, a mixture of methylchlorosilanes dominated by $SiH(CH_3)Cl_2$ along with CH_4 is generated and then fed into the tail gas system. This will provide the necessary theoretical foundation for the development of efficient and low-cost impurity removal strategies.

Keywords: polysilicon; carbon impurities; existing forms; evolution mechanism; HSC simulation calculations

Check for updates

Academic Editor: Fabrizio Roccaforte

Received: 17 December 2025
Revised: 9 February 2026
Accepted: 14 February 2026
Published: 18 February 2026

Copyright: © 2026 by the authors. Licensee MDPI, Basel, Switzerland. This article is an open access article distributed under the terms and conditions of the Creative Commons Attribution (CC BY) license.

1. Introduction

The growing global demand for energy, coupled with the increasing severity of the greenhouse effect, has accelerated the formation of a new global energy system and facilitated the transition of the global energy system toward low carbonization. New types of green energy, represented by wind power and photovoltaic energy, are poised to embrace new historical development opportunities. High-purity polysilicon is a critical foundational material for the photovoltaic and semiconductor industries, and it is of great significance to the green and high-quality development of the global energy and information sectors. It is mainly produced via the silane fluidized bed process and the improved Siemens method [1–4]. During the formation of single crystal silicon, carbon impurities in polysilicon will accelerate the formation of oxygen precipitates, thereby inducing secondary defects

such as dislocations and stacking faults, affecting the minority carrier lifetime and the lattice arrangement of monocrystalline silicon. These impurities are one of the key factors restricting the photoelectric conversion efficiency of solar cells [1,3,5].

Constructing low-cost and highly selective targeted removal strategies to replace the "one-size-fits-all" broad-spectrum removal mode adopted by traditional impurity removal processes, thus effectively regulating carbon impurities at different stages, is of great significance for breaking through the purity bottleneck of polysilicon and reducing the energy consumption and costs of purification. Systematic clarification of the existing forms and evolution mechanisms of carbon impurities is a necessary foundation for the construction of highly selective targeted strategies. Researchers have conducted extensive studies focusing on the sources, detection and analysis methods, and physical property parameters of carbon impurity compounds, thus yielding a series of innovative achievements. For example, Yuan [6], in summarizing the sources of impurities during the preparation of electronic-grade polysilicon from industrial silicon, proposed control strategies from the aspects of raw material preparation, purification, impurity inhibition mechanisms in the trichlorosilane ($SiHCl_3$) separation process, and tail gas separation technologies, and concluded that impurities in high-purity polysilicon are mainly derived from recycled hydrogen, $SiHCl_3$ (metallic silicon), graphite electrodes, equipment pipelines, gaskets, and the environment. Based on the analysis results of carbon impurity sources, transformation, and raw material purification, Cao et al. [7] proposed that the carbon impurity concentration in high-purity $SiHCl_3$ can be reduced by controlling the carbon impurity concentration in metallurgical silicon and applying the optimal purification technology; meanwhile, the purity of polysilicon can be improved through the coordinated control of the methane (CH_4) concentration in recovered hydrogen. Chen [8] employed gas chromatography–mass spectrometry (GC-MS) to analyze the speciation of polychlorosilanes and methylchlorosilanes in synthetic chlorosilanes (produced via direct chlorination), and concluded that carbon impurities in synthetic chlorosilanes are primarily composed of monomethyldichlorosilane ($SiH(CH_3)Cl_2$), dimethyldichlorosilane ($Si(CH_3)_2Cl_2$), and methyltrichlorosilane ($Si(CH_3)Cl_3$). Yang [9] established a rapid determination method (GC-MS) for $SiH(CH_3)Cl_2$, trimethylchlorosilane ($Si(CH_3)_3Cl$), $Si(CH_3)Cl_3$, and $Si(CH_3)_2Cl_2$ in high-purity $SiHCl_3$ using 1,2-dichloroethane as the internal standard. The detection limit and reproducibility of this method can meet the testing requirements for carbon impurities in $SiHCl_3$ used in polysilicon production, and it has also become a universally adopted method in the industry at present. Lewis et al. [10] reported gas chromatography and infrared spectroscopy analytical methods related to carbon impurities in chlorosilanes. Coleman et al. [11] identified the possible existing forms of impurities in chlorosilanes and separately provided key property parameters of the relevant compounds, such as saturated vapor pressure equations, boiling points, critical temperatures, critical pressures, and critical volumes, aiming to provide a basis for the simulation calculation of rectification columns and their operating parameters. Vaisarová [12] provided the dipole moments of chlorine-containing organosilicon compounds, which will serve as a basis for the selection of adsorbents. In addition to the aforementioned studies, research on carbon impurities also covers aspects such as the transformation of carbon-containing compounds in $SiHCl_3$ [10,13–16], and the impact of CH_4 content in hydrogen on the quality of polysilicon [6]. However, the content of carbon impurities in raw materials is at a trace level, affected by the detection limits of testing equipment and the stability of compounds, so the accurate characterization of the existing forms and evolution processes of carbon impurities at different stages is limited, and existing detection technologies cannot achieve the accurate detection of all compounds. Owing to the influence of the reaction conditions of the Si-H-Cl system, it is extremely challenging to achieve the online detection of all carbon

impurity-related elements and compounds. No hydrocarbon compounds such as ethane, CO and CO_2, have been detected in hydrogen; and no tetramethylsilane, monomethylmonochlorosilane and other such substances have been detected in chlorosilanes. However, it is necessary to further clarify their presence, given that these substances exert a significant impact on intermediate products and high-purity polysilicon.

Based on the above understanding, this paper starts from the key processes of polysilicon production (direct chlorination, cold hydrogenation, and reduction reaction), combines thermodynamic calculation and experimental characterization methods, and analyzes the dominant existing forms and evolution driving forces of carbon impurities at each stage, as well as the evolution rules of carbon impurities during polysilicon production. This will provide a theoretical basis for the development of phased targeted impurity removal strategies and the improvement in polysilicon quality and reduction in cost.

2. Materials and Methods

2.1. Thermodynamic Calculation Modeling Methods

Gibbs free energy is a crucial thermodynamic function, typically employed to determine the direction and extent of a reaction under specific temperature and pressure conditions. Generally, the lower the Gibbs free energy of a reaction, the greater the driving force of the spontaneous reaction, and the more spontaneously the reaction proceeds [17].

HSC Chemistry (version: HSC 6.0) is a simulation software based on fundamental concepts of chemical thermodynamics, designed to calculate thermodynamic parameters of substances under ideal conditions. The commonly used functions of HSC Chemistry include the calculation of thermodynamic parameters for chemical reactions, heat and material balance calculations, electrochemical equilibrium calculations, and Pourbaix diagram plotting, among others. A key advantage of this software is that it eliminates the need to consider the kinetics of chemical reactions and the non-ideality of solutions, enabling the efficient and convenient verification of the thermodynamic validity of reaction equations involving arbitrary reactants and products, along with the calculation of their corresponding thermodynamic parameters. Thus, it is typically applied in the calculation of thermodynamic parameters for chemical reactions, heat and material balance calculations, etc. In accordance with the laws of thermodynamics, the Gibbs free energy of a reaction is closely correlated with the equilibrium constant and the equilibrium composition of species. In this work, the reaction equation module of the HSC simulation software (HSC 6.0, Metso Finland Oy, Espoo, Finland) was employed to compute the Gibbs free energy of the relevant reactions [18], so as to predict the tendency of formation of the corresponding reaction products.

2.2. Materials and Experiments

The metallurgical silicon (≥99%), polysilicon (≥99.99999999), $SiHCl_3$, silicon tetrachloride ($SiCl_4$), and recycled hydrogen (≥99.9%), were supplied by Xinjiang Xinte Crystalline Silicon High-Tech Co., Ltd. (Urumqi, China). The carbon content in metallurgical silicon was determined using the infrared absorption method (carbon-sulfur analyzer, SC-2800, NCS Testing Technology Co., Ltd., Beijing, China) [19], high-frequency heating and pure oxygen combustion were employed, with a sample mass of 1.5 g per test run and three replicate samples prepared for each sample. The carbon impurity contents in $SiHCl_3$ and $SiCl_4$ were measured via chromatography–mass spectrometry (GC-MS, 8850-5977, Agilent Technologies, Inc., Santa Clara, CA, USA) [20], the type of column used in this work was DB-VRX, the carrier gas was He; for the heating program, the initial temperature was set at 40 °C and held for 16 min, then ramped up to 200 °C at a rate of 50 °C/min and held for 1 min for detection. The actual value was determined as the average of the initial

test values obtained from three replicate samples. For recycled hydrogen, the carbon impurity content was analyzed by gas chromatography (GC, SC-8100, Chongqing Chuanyi Automation Co., Ltd., Chongqing, China) [21]. The phase compositions of metallurgical silicon and polysilicon were characterized using an X-ray diffractometer (XRD, Smart Lab 9 kW, Rigaku Corporation, Hokuto City, Yamanashi Prefecture, Japan) [22], using CuKα radiation at a scan rate of 2°/min. In this study, Bragg–Brentano diffraction geometry was adopted to achieve a mechanical coupling motion mode with a 1:2 angular ratio of θ to 2θ. The variation curve of diffraction intensity as a function of the 2θ angle was automatically captured and recorded, thereby generating the corresponding X-ray diffraction (XRD) patterns. For silicon powder and polycrystalline silicon, two replicate samples were tested for each material, and the results obtained were almost identical. Therefore, one representative diffraction pattern from each was selected for presentation in this paper, and the phase composition was analyzed on the basis of the standard single-phase PDF cards. Furthermore, due to the low carbon impurity content in polysilicon, polysilicon was fabricated into single crystal ingots via the floating zone (FZ) melting technique in accordance with the national standard GB/T 29057 [23]. Subsequently, the carbon content was measured using a cryogenic Fourier transform infrared spectrometer (CryoSAS, Bruker Corporation, Ettlingen, Germany) [24].

3. Results and Discussion

3.1. Technological Route for Polysilicon Preparation via the Modified Siemens Process

The technology route of the modified Siemens process is shown in Figure 1. Under specific temperature (540–560 °C) and pressure (2.5–3.5 MPa) conditions, metallurgical silicon, hydrogen, and $SiCl_4$ undergo a chemical reaction to generate a chlorosilane mixture (via cold hydrogenation, with the remainder supplemented by the reaction of metallurgical silicon and hydrogen chloride (HCl, direct chlorination, 280~320 °C, 0.25~0.30 MPa). Subsequently, a series of purification and separation steps are conducted to obtain high-purity refined $SiHCl_3$ (distillation process). The refined $SiHCl_3$ is then fed into a reduction furnace (reduction process), where it undergoes a chemical vapor deposition (CVD, 1000~1100 °C, 0.6 MPa) reaction with high-purity hydrogen to produce polysilicon. Meanwhile, a comprehensive tail gas recovery system is equipped to ensure the full utilization of materials (tail gas recovery process), thereby achieving the closed-loop production of polysilicon. The main introduction points of carbon impurities in polysilicon are cold hydrogenation (direct chlorination), CVD, and tail gas recovery, with the primary material sources being metallurgical silicon, $SiCl_4$, $SiHCl_3$, and recovered hydrogen.

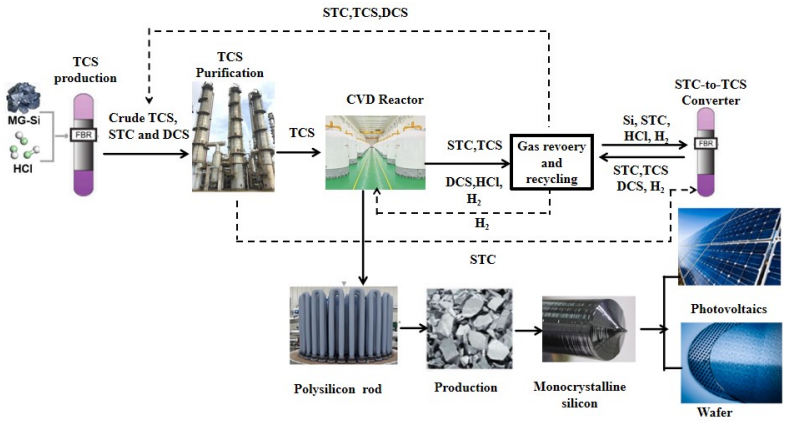


Figure 1. Technological route for polysilicon preparation via the modified Siemens process and its applications.

3.2. Existence Forms of Carbon Impurities in Metallurgical Silicon and Polysilicon

Literature studies have indicated that metallurgical silicon is one of the primary source of carbon impurities in high-purity electronic-grade polysilicon [6]. Therefore, in this work, X-ray diffraction (XRD) technology was employed to characterize the phase compositions of metallurgical silicon and polysilicon powder, aiming to determine the existence forms of carbon impurities, as illustrated in Figure 2. Characteristic diffraction peaks associated with silicon (ICCD PDF-4 + 04-001-7247) were detected in the XRD patterns of both metallurgical silicon powder and polysilicon powder. The 2θ values at 28.4°, 47.3°, 56.1°, 69.2° and 76.4° correspond to the (111), (220), (311), (400) and (331) crystal planes of elemental silicon, respectively. In terms of phase composition, no obvious difference was observed between the two powders, except for the intensity variations in the diffraction peaks from different crystal planes. No characteristic peaks related to carbon-containing impurity phases were identified, which might be ascribed to the detection limit of the XRD method. Figure 3 shows the Raman spectra of metallurgical silicon and polysilicon, The characteristic peaks at wavenumbers of 520 cm^{-1} and 960 cm^{-1} are associated with the fundamental and overtone frequencies of the stretching vibration of the Si-Si bond, respectively. Similar to XRD, no characteristic peaks associated with C (1350 cm^{-1} and 1580 cm^{-1}) and SiC (777 cm^{-1}, 799 cm^{-1}, 802 cm^{-1} and 905 cm^{-1}) were observed in the Raman spectra of metallurgical silicon and polycrystalline silicon.

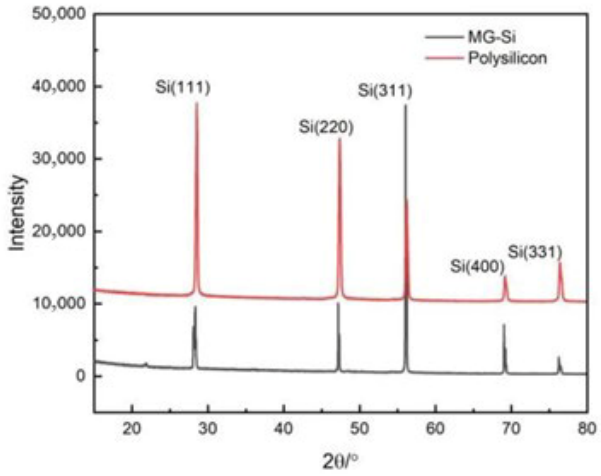


Figure 2. Phase composition of metallurgical silicon and polysilicon.

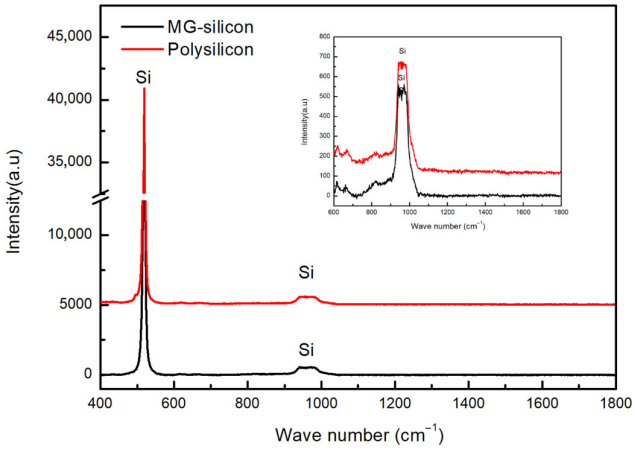


Figure 3. Raman spectra of metallurgical silicon and polysilicon.

In this work, six metallurgical silicon samples and six polysilicon powder samples were selected, and their carbon contents were determined using a carbon-sulfur analyzer. The results showed that the carbon impurity content in the six metallurgical silicon samples was 0.012~0.023%, while the carbon impurity contents in the six polysilicon powder samples were all below the detection limit of the method (0.01%) and thus not detected. Furthermore, the floating zone (FZ) crystal growth method combined with cryogenic infrared spectroscopy was employed to measure the carbon impurity content in the six polysilicon samples. The results indicated that the carbon impurity content in the six single crystal silicon samples was 22~36 ppb (Table 1). Compared with the minimum concentration threshold for silicon carbide formation at the melting point of silicon (approximately 65 ppm; exceeding this value results in the formation of silicon carbide compounds in the melt) [25,26], the carbon impurity concentration in metallurgical silicon powder (denoted as C_{MG-si}) is higher, while the carbon impurity concentration in high-purity polysilicon (denoted as C_{EG-si}) is lower. In other words, the minimum concentration threshold for the formation of silicon carbide compounds in the silicon melt (C_{mc}, 65 ppm) lies between the carbon impurity concentrations of metallurgical silicon powder and polysilicon ($C_{MG-si} > C_{mc} > C_{EG-si}$). Therefore, in metallurgical silicon powder, the main existing forms of carbon impurities are a mixture of dissolved carbon atoms and silicon carbide, whereas in polysilicon, carbon impurities mainly exist in the form of dissolved atoms.

Table 1. Carbon impurity concentrations in metallurgical-grade silicon and polysilicon.

Metallurgical-Grade Silicon	Sample	1	2	3	4	5	6
	Concentration (%)	0.015	0.023	0.012	0.018	0.015	0.021
Polysilicon	Sample	1	2	3	4	5	6
	Concentration (ppb)	26	36	29	34	30	22

3.3. Evolution of Carbon Impurities and HSC Simulation of Reaction Thermodynamics

$SiHCl_3$ is the main raw material for producing polysilicon. It is mainly prepared by cold hydrogenation technology, with the rest supplemented by direct synthesis. Therefore, the main sources of carbon impurities in $SiHCl_3$ include metallurgical silicon, hydrogen gas, and $SiCl_4$. According to the literature report during the processes of direct synthesis and cold hydrogenation reactions, silicon carbide in metallurgical silicon has no reaction activity, and the substances that participate in the reaction are the dissolved carbon atoms in metallurgical silicon [27]. The reaction system is mainly composed of elemental silicon, dichlorosilane (SiH_2Cl_2), $SiHCl_3$, $SiCl_4$, hydrogen, HCl, and corresponding impurities. SiH_2Cl_2, $SiHCl_3$, $SiCl_4$, hydrogen and HCl undergo cleavage, generating free radicals such as $SiCl_2\cdot$, $SiCl_3\cdot$, $Cl\cdot$, $H\cdot$, $SiHCl_2\cdot$, and $SiHCl\cdot$. Subsequently, the free radical rearrangement occurs, producing the reaction products (SiH_2Cl_2 and $SiHCl_3$) [10,28]. During this process, the solid solution carbon atoms in the metallurgical silicon react with hydrogen to produce CH_4. A portion of the CH_4 undergoes cracking to generate $CH_3\cdot$ free radicals. Additionally, the methylchlorosilane compounds in chlorosilane and the CH_4 in the recycled hydrogen also crack, leading to the formation of $CH_3\cdot$ free radicals. The $CH_3\cdot$ free radicals combine with $Cl\cdot$ free radicals to form chloromethane (CH_3Cl), which then reacts with elemental silicon to generate methylchlorosilanes in different forms (Rochow reaction). Meanwhile, the methyl radicals ($CH_3\cdot$) combine with silicon-containing radicals including $SiCl_2\cdot$, $SiCl_3\cdot$, $SiHCl_2\cdot$, $SiHCl\cdot$ and hydrogen radicals ($H\cdot$), forming a mixture of methylchlorosilanes and CH_4 [10,29].

The raw materials for the direct chlorination process are metallurgical silicon and HCl. The chlorine-containing substances in the reaction system include HCl, $SiHCl_3$,

SiH_2Cl_2, $SiCl_4$, as well as the chlorides generated by the reaction between impurities in metallurgical silicon and chlorine-containing substances. Under certain conditions, carbon impurities in the metallurgical silicon can be converted into carbon-containing organic impurities, such as $SiH(CH_3)Cl_2$, $Si(CH_3)_3Cl$, $Si(CH_3)Cl_3$, $Si(CH_3)_2Cl_2$, and undetectable organosilanes. Gibbs free energy is a thermodynamic parameter for evaluating the direction and extent of chemical reactions, and it is a state function. Its value is only related to the initial and final states of reactants and products, rather than the process path. Therefore, this paper uses the Gibbs free energy of the overall reaction to determine spontaneity. The possible reactions of carbon impurities and their corresponding Gibbs free energy values are shown in Table 2 and Figure 4. It can be seen that in the absence of a chlorine source, the Gibbs free energy of the reaction between carbon, silicon and hydrogen is positive. This means the reaction is non-spontaneous, and no $Si(CH_3)_4$ is generated in the system. When HCl is used as the chlorine source, silicon, carbon, hydrogen, and HCl react to form a silicone mixture. Among these reactions, the Gibbs free energy for the formation of $Si(C_6H_5)Cl_3$ is nearly zero, resulting in a low reaction driving force. All other reactions proceed spontaneously, specifically, the reactions producing $Si(CH_3)Cl_3$ and $SiH(CH_3)Cl_2$ have lower Gibbs free energy and thus higher reaction driving forces. The chemical reaction between $SiCl_4$, hydrogen, and carbon is non-spontaneous, which is similar to that of $SiHCl_3$. The reaction between SiH_2Cl_2, carbon, and hydrogen produces $SiH(CH_3)Cl_2$, but does not generate $Si(CH_3)_3Cl$. The reactions between CH_4, and $SiHCl_3$ as well as $SiCl_4$ are non-spontaneous. $Si(CH_3)Cl_3$ reacts spontaneously with hydrogen to produce CH_4 and $SiHCl_3$, while the reaction between $SiH(CH_3)Cl_2$ and hydrogen is non-spontaneous. $Si(CH_3)Cl_3$ reacts spontaneously with both $SiHCl_3$ and SiH_2Cl_2, and all reactions produce $SiH(CH_3)Cl_2$. $SiH(CH_3)Cl_2$ undergoes a spontaneous reaction with HCl, producing CH_4 and $SiHCl_3$. $Si(CH_3)Cl_3$ can undergo a decomposition reaction to form $Si(CH_3)_3Cl$ and $SiCl_4$. However, the decomposition reactions of $SiH(CH_3)Cl_2$ and CH_4 are non-spontaneous. In the direct chlorination reaction system, the order of Gibbs free energy for spontaneous reactions is $\Delta G_{20} < \Delta G_3 < \Delta G_2 < \Delta G_{19} < \Delta G_{22} < \Delta G_{18} < \Delta G_8 < \Delta G_{17} < \Delta G_4 < \Delta G_{21}$. Among reactions of the same type, the Gibbs free energy for the reaction generating $SiH(CH_3)Cl_2$ is lower. Additionally, the reaction of $Si(CH_3)Cl_3$ with chlorosilanes to form $SiH(CH_3)Cl_2$ is spontaneous, which indicates that $SiH(CH_3)Cl_2$ is more likely to form. Although the Gibbs free energy of Reaction 22 is relatively low, the content of $SiCl_4$ is much higher than that of $Si(CH_3)Cl_3$; therefore, the concentration of $Si(CH_3)_3Cl$ is relatively low. The Gibbs free energy of Reaction 25 is positive, indicating that polyatomic hydrocarbon compounds such as ethane cannot exist stably in this system. The Gibbs free energy of Reactions 26 to 29 is negative, meaning that methane and elemental carbon are more prone to form under hydrogen-rich conditions when carbon monoxide and carbon dioxide are present in hydrogen gas. In summary, in the direct chlorination reaction system, the main existing forms of carbon impurities are $SiH(CH_3)Cl_2$ and CH_4, accompanied by trace amounts of $Si(CH_3)_3Cl$ and $Si(CH_3)Cl_3$.

Since the material system involved in the cold hydrogenation reaction is basically similar to that of direct chlorination, with only differences in the proportions of $SiHCl_3$ and $SiCl_4$ and in the reaction temperature, the spontaneity of the relevant reactions is similar to that of direct chlorination. The difference, however, is that the Gibbs free energy of Reaction 4 changes from a negative value to a positive value, and the order of the magnitudes of the Gibbs free energy for spontaneous reactions becomes $\Delta G_{20} < \Delta G_{22} < \Delta G_{19} < \Delta G_3 < \Delta G_{18} < \Delta G_{17} < \Delta G_8 < \Delta G_2 < \Delta G_{21}$. This results in the product composition and the main existing forms of carbon impurities being similar to those in the direct chlorination reaction.

Table 2. Possible reactions of carbon impurities and their Gibbs free energy during the direct chlorination process.

No.	Reaction Equation	ΔG (kcal/mol)						
		25 °C	280 °C	320 °C	540 °C	560 °C	1000 °C	1100 °C
1	$Si + 4C + 6H_2(g) = Si(CH_3)_4(g)$	−35.39	10.53	16.05	26.91	29.44	97.24	107.47
2	$Si + C + 3HCl(g) = Si(CH_3)Cl_3(g)$	−43.54	−29.10	−26.82	−14.34	−13.20	11.53	17.11
3	$Si + C + 2HCl(g) + H_2(g) = SiH(CH_3)Cl_2(g)$	−44.03	−31.51	−29.50	−18.46	−17.45	4.16	8.92
4	$Si + 3C + HCl(g) + 4H_2(g) = Si(CH_3)_3Cl(g)$	−35.28	−10.99	−7.07	14.68	16.67	59.87	69.46
5	$Si + 6C + 3HCl(g) + H_2(g) = Si(C_6H_5)Cl_3(g)$	−22.75	−2.63	0.55	18.09	19.69	54.47	62.45
6	$SiCl_4(g) + C + 3H_2(g) = SiH(CH_3)Cl_2(g) + 2HCl(g)$	13.61	15.87	16.31	18.95	19.20	24.69	25.84
7	$SiCl_4(g) + 3C + 6H_2(g) = Si(CH_3)_3Cl(g) + 3HCl(g)$	22.37	36.40	38.80	52.55	53.84	80.40	86.36
8	$SiH_2Cl_2(g) + C + H_2(g) = SiH(CH_3)Cl_2(g)$	−19.10	−13.29	−12.32	−7.13	−6.69	3.44	5.61
9	$SiH_2Cl_2(g) + 3C + 4H_2(g) = Si(CH_3)_3Cl(g) + HCl(g)$	−10.35	7.26	10.11	26.01	27.47	59.15	66.14
10	$SiHCl_3(g) + C + H_2(g) = Si(CH_3)Cl_3(g)$	−0.77	5.45	6.45	12.03	12.54	23.87	26.45
11	$SiHCl_3(g) + C + 2H_2(g) = SiH(CH_3)Cl_2(g) + HCl(g)$	−1.26	3.04	3.78	7.91	8.29	16.51	18.42
12	$SiHCl_3(g) + 3C + 5H_2(g) = Si(CH_3)_3Cl(g) + 2HCl(g)$	7.49	23.56	26.21	41.05	42.42	72.88	78.8
13	$SiHCl_3(g) + CH_4(g) = SiH(CH_3)Cl_2(g) + HCl(g)$	10.81	9.59	9.38	8.90	7.97	4.80	3.94
14	$SiCl_4(g) + CH_4(g) = Si(CH_3)Cl_3(g) + HCl(g)$	26.18	24.82	24.58	23.26	23.13	20.36	19.72
15	$SiCl_4(g) + 3CH_4(g) = Si(CH_3)_3Cl(g) + 3HCl(g)$	58.60	56.04	55.56	52.65	52.37	45.30	43.43
16	$SiH(CH_3)Cl_2(g) + H_2(g) = CH_4(g) + SiH_2Cl_2(g)$	7.03	6.71	6.71	6.94	6.98	8.26	8.71
17	$Si(CH_3)Cl_3(g) + H_2(g) = CH_4(g) + SiHCl_3(g)$	−11.31	−12.00	−12.05	−12.22	−12.23	−12.17	−12.14
18	$Si(CH_3)Cl_3(g) + SiHCl_3(g) = SiH(CH_3)Cl_2(g) + SiCl_4(g)$	−15.37	−15.22	−15.21	−15.16	−15.16	−15.56	−15.78
19	$Si(CH_3)Cl_3(g) + SiH_2Cl_2(g) = SiH(CH_3)Cl_2(g) + SiHCl_3(g)$	−18.33	−18.71	−18.77	−19.16	−19.20	−20.43	−20.85
20	$2Si(CH_3)Cl_3(g) + SiH_2Cl_2(g) = 2SiH(CH_3)Cl_2(g) + SiCl_4(g)$	−33.71	−33.93	−33.98	−34.32	−34.36	−35.98	−36.62
21	$SiH(CH_3)Cl_2(g) + HCl(g) = CH_4(g) + SiHCl_3(g)$	−10.81	−9.60	−9.38	−8.09	−7.97	−4.84	−3.94
22	$3Si(CH_3)Cl_3(g) = Si(CH_3)_3Cl(g) + 2SiCl_4(g)$	−19.96	−18.42	−18.21	−17.12	−17.03	−15.76	−15.73
23	$3SiH(CH_3)Cl_2(g) = Si(CH_3)_3Cl(g) + SiHCl_3(g) + SiH_2Cl_2(g)$	29.12	30.73	30.98	32.37	32.50	35.76	36.67
24	$CH_4(g) = C + 2H_2(g)$	12.08	6.55	5.60	0.18	−0.32	−11.70	−14.31
25	$2CH_4(g) = C_2H_6(g) + H_2(g)$	16.30	16.81	16.86	16.95	16.95	16.80	16.75
26	$CO(g) + H_2(g) = C + H_2O(g)$	−21.85	−13.42	−12.07	−4.59	−3.90	11.16	14.57
27	$CO_2(g) + 2H_2(g) = C + 2H_2O(g)$	−15.01	−9.03	−8.04	−2.43	−1.93	9.82	12.54
28	$CO(g) + 3H_2(g) = CH_4(g) + H_2O(g)$	−33.92	−19.97	−17.68	−4.78	−3.59	22.86	28.90
29	$CO_2(g) + 4H_2(g) = CH_4(g) + 2H_2O(g)$	−27.08	−15.58	−13.65	−3.65	−2.62	21.52	26.86
30	$CO_2(g) + Si = C + SiO_2$	−110.44	−99.15	−97.39	−87.85	−86.99	−68.61	−64.52
31	$2CO(g) + Si = 2C + SiO_2$	−139.12	−116.96	−113.50	−94.59	−92.89	−56.11	−47.90

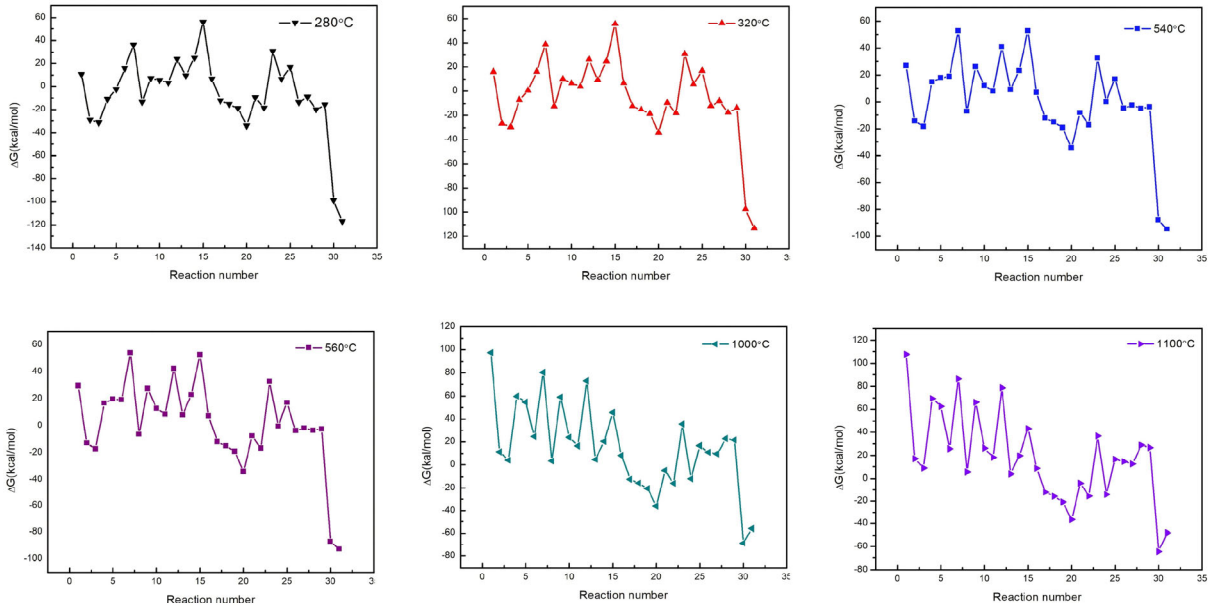


Figure 4. Gibbs free energy of reactions 1–31 at different temperatures.

The distillation process mainly focuses on the separation of the main components (SiH_2Cl_2, $SiHCl_3$ and $SiCl_4$) and the purification of $SiHCl_3$. Meanwhile, it is accompanied by the redistribution and enrichment of methylchlorosilanes in different components, but does not involve the conversion between different compounds. Since the boiling point of $SiH(CH_3)Cl_2$ (41–42 °C) is close to that of $SiHCl_3$ (31.2 °C), and the boiling point of $SiCl_4$ (57.6 °C) lies between those of $SiH(CH_3)Cl_2$ and $Si(CH_3)Cl_3$ (66 °C), after rough distillation separation, $SiH(CH_3)Cl_2$ is enriched in $SiHCl_3$ (at the top of the tower), while $Si(CH_3)Cl_3$ is enriched in $SiCl_4$ (at the bottom of the tower); in addition, the bottom product also contains a small amount of $SiH(CH_3)Cl_2$. After multiple rounds of distillation purification, $SiH(CH_3)Cl_2$ becomes the main impurity in the refined $SiHCl_3$. Since the boiling point of CH_4 is much lower than that of chlorosilanes, CH_4 enters the hydrogen recovery system.

In the reduction process, the main raw materials are high-purity $SiHCl_3$ (containing a small amount of SiH_2Cl_2) and hydrogen. The products include HCl, Si, $SiCl_4$, SiH_2Cl_2, along with unreacted hydrogen and $SiHCl_3$. That is, the main material system is Si-Cl-H, which is similar to the cold hydrogenation reaction. The main existing forms of carbon impurities in the raw materials are $SiH(CH_3)Cl_2$ and CH_4. Concurrent with the reactions of the main material system, free radical generation and rearrangement reactions similar to those occurring in the cold hydrogenation process also take place, producing CH_4 and methylchlorosilanes. Meanwhile, CH_4 cracking reactions occur, which generate methyl free radicals and elemental carbon [30,31]. The reactions between carbon impurities and the main material system, along with their Gibbs free energy, are shown in Table 3.

Table 3. Detection results of carbon impurities in crude chlorosilane produced by the direct chlorination process and cold hydrogenation process (ppm).

Sample No	CH_3SiHCl_2		CH_3SiCl_3		$(CH_3)_3SiCl$		$(CH_3)_2SiCl_2$	
	DC	HC	DC	HC	DC	HC	DC	HC
1	1.02×10^3	1.65	121	30.8	/	/	/	/
2	1.03×10^3	1.18	131	242	/	/	/	/
3	1.17×10^3	1.40	192	176	/	/	/	/
4	1.14×10^3	1.33	150	83.1	/	/	/	/
5	1.17×10^3	2.52	82.3	24.5	/	/	/	/
6	901	3.22	71.2	47.5	/	/	/	/
7	927	14.5	87.7	255	/	/	/	/
8	1.09×10^3	8.14	92.5	2.04	/	/	/	/
9	1.39×10^3	6.04	121	107	/	/	/	/
10	1.36×10^3	5.31	44.4	84.5	/	/	/	/

Note: "/" indicates not detected, meaning the concentration is below the detection limit (1 ppm), DC and HC represent direct chlorination and cold hydrogenation, respectively.

Carbon (graphite) is one of the important sources of carbon impurities in polysilicon. Carbon atoms diffuse from graphite electrodes into the root of polysilicon rods, thereby forming carbon-headed silicon [3,6,7]. At 1000~1100 °C, in the coexistence of silicon and carbon, the Gibbs free energy of the reactions between them with H_2, HCl, and chlorosilanes to form methylsilane, methylchlorosilanes, and phenylchlorosilanes is positive. These forward reactions are non-spontaneous, indicating that methylchlorosilanes are unstable in the reduction system and prone to decomposing into elemental carbon. The Gibbs free energy of the reactions between chlorosilane and CH_4 as well as between $SiH(CH_3)Cl_2$ and hydrogen is positive, indicating that these reactions are non-spontaneous in the forward direction. In contrast, the Gibbs free energy values for the reactions of $Si(CH_3)Cl_3$ with hydrogen and of $SiH(CH_3)Cl_2$ with HCl to form CH_4 are negative, meaning these reactions proceed spontaneously forward. Additionally, the reactions between $Si(CH_3)Cl_3$ and

chlorosilane to generate $SiH(CH_3)Cl_2$ also exhibit negative Gibbs free energy, confirming their spontaneity. These thermodynamic characteristics provide favorable conditions for the existence of CH_4 and $SiH(CH_3)Cl_2$ in the system. The Gibbs free energy for the decomposition of $Si(CH_3)Cl_3$ to form $Si(CH_3)_3Cl$ is negative, whereas the Gibbs free energy for the decomposition of $SiH(CH_3)Cl_2$ to form $Si(CH_3)_3Cl$ is positive. Combined with the high concentration of $SiCl_4$ in the system, these results indicate that trace amounts of $Si(CH_3)_3Cl$ may exist in the system. The Gibbs free energy of all reactions leading to the formation of $Si(CH_3)Cl_3$ is positive, indicating that $Si(CH_3)Cl_3$ cannot exist stably in the system. Under hydrogen-rich conditions, the Gibbs free energy for the formation of ethane (alkane, Reaction 25) via methane decomposition is positive, indicating that no other hydrocarbon compounds apart from methane are generated in the reaction system. It can be concluded from the Gibbs free energy of the reaction that CH_4 tends to decompose to generate elemental carbon in the reduction system. Given the low concentrations of CH_4 impurities in high-purity hydrogen and $SiH(CH_3)Cl_2$ impurities in $SiHCl_3$, and considering that the solubility of carbon in silicon melt is approximately 65 ppm, carbon exists in high-purity polysilicon in the form of solute atoms. Unlike the direct chlorination and cold hydrogenation systems, the Gibbs free energy values of the reduction reactions of carbon monoxide and carbon dioxide (Reactions 26 to 29) are dominant in the CVD system. However, the Gibbs free energy values of Reactions 30 and 31 are negative, meaning that carbon monoxide and carbon dioxide tend to be reduced by elemental silicon to form silicon dioxide and elemental carbon. In other words, carbon monoxide and carbon dioxide cannot exist stably in this system. In summary, the main existing forms of carbon-related impurities in the reduction system are solute carbon atoms, CH_4, and $SiH(CH_3)Cl_2$, accompanied by a small amount of $Si(CH_3)_3Cl$.

When producing high-purity polysilicon using the improved Siemens process, the recovered hydrogen mainly consists of two parts: reduction-recovered hydrogen and hydrogenation-recovered hydrogen. After separation and purification treatment, the reduction-recovered hydrogen is fed into the CVD system for recycling, with the regenerated hydrogen entering the cold hydrogenation system. The hydrogenation-recovered hydrogen is fed into the cold hydrogenation system for recycling, with the regenerated hydrogen discharged as waste gas. In the condensation and absorption/desorption process (tail gas recovery process), hydrogen in the tail gas is separated from chlorosilanes and HCl. High-boiling compounds such as chlorosilanes and methylchlorosilanes are fed into the subsequent distillation system, while HCl is absorbed by chlorosilanes. Low-boiling-point compounds such as hydrogen are introduced into the reduction or cold hydrogenation system. Compared with methylchlorosilanes, CH_4 has a lower boiling point (-161.5 °C), and thus it enters the reduction and cold hydrogenation units along with hydrogen. In contrast, methylchlorosilanes follow chlorosilanes into the distillation process for further separation. Consequently, the carbon impurities in the recovered hydrogen are mainly in the form of CH_4.

3.4. Sampling and Analysis Results of Carbon-Containing Materials at Different Sites

To verify the reliability of the above simulation results, this work conducted test and analysis on chlorosilane and hydrogen at key positions, in addition to metallurgical silicon and high-purity polysilicon. Among the results, Table 3 presents the analysis results of carbon impurities in crude chlorosilane generated by the synthesis process. It can be seen from the table that for the crude chlorosilane from the direct chlorination process (with a $SiHCl_3$ content of $\geq$85%), the carbon impurities are mainly composed of CH_3SiHCl_2, with a small amount of $Si(CH_3)Cl_3$, while $(CH_3)_3SiCl$ and $(CH_3)_2SiCl_2$ are not detected. Before distillation separation, in the chlorosilane generated by the cold hydrogenation

process (with a $SiHCl_3$ content of approximately 27–29%), the carbon impurities mainly exist in the form of CH_3SiHCl_2 and $Si(CH_3)Cl_3$. $(CH_3)_3SiCl$ and $(CH_3)_2SiCl_2$ are not detected (Table 3). In contrast to the crude trichlorosilane ($SiHCl_3$) produced in the direct chlorination synthesis process, the product herein has a higher content of $Si(CH_3)Cl_3$, which is mainly attributed to the high concentration of $Si(CH_3)Cl_3$ in the silicon $SiCl_4$ feedstock.

Whether by direct chlorination or cold hydrogenation process, it is necessary to subject the chlorosilane mixture to crude distillation and separation treatment. The overhead product of the crude distillation column is further purified to obtain high-purity refined $SiHCl_3$, which is then fed into the reduction system, while the bottom product $SiCl_4$ is sent to the cold hydrogenation system for recovery and reuse. This study conducted a carbon impurity test and analysis on the purified $SiHCl_3$ entering the reduction process, and the results are shown in Table 4. In the purified $SiHCl_3$, carbon impurities mainly exist in the form of CH_3SiHCl_2, and other carbon-containing compounds are not detected. This study also tested the carbon impurities in the bottom product (mainly composed of $SiCl_4$) after the crude separation of chlorosilane produced by cold hydrogenation, and the results are shown in Table 4. In the chlorosilane at the bottom of the crude distillation column, carbon impurities are mainly composed of $Si(CH_3)Cl_3$, with a small amount of CH_3SiHCl_2 also present.

Table 4. Analysis results of carbon impurities in purified trichlorosilane and chlorosilane at the bottom of the crude distillation column (ppm).

Sample No	CH_3SiHCl_2		CH_3SiCl_3		$(CH_3)_3SiCl$		$(CH_3)_2SiCl_2$	
	Purified TCS	STC	Purified TCS	STC	Purified TCS	STC	Purified TCS	STC
1	7.22	/	/	195	/	/	/	/
2	9.03	1.17	/	544	/	/	/	/
3	8.21	/	/	214	/	/	/	/
4	2.82	/	/	254	/	/	/	/
5	5.84	1.73	/	649	/	/	/	/
6	3.18	/	/	175	/	/	/	/
7	7.87	1.48	/	766	/	/	/	/
8	3.51	1.22	/	735	/	/	/	/
9	5.03	1.07	/	699	/	/	/	/
10	3.91	1.54	/	764	/	/	/	/

Note: Purified TCS and STC represent direct chlorination and chlorosilane at the bottom of the crude distillation column, respectively.

In this work, 10 samples of reduction-recovered hydrogen and 10 samples of hydrogenation-recovered hydrogen were selected, and their carbon impurity compositions were tested. The results are shown in Table 5; the carbon impurities in the two types of recovered hydrogen mainly exist in the form of CH_4. No other forms of carbon-containing compounds are detected, and the CH_4 content in the hydrogenation-recovered hydrogen is higher. In conclusion, after separation treatment via rectification and tail gas recovery processes, carbon impurities mainly exist in the forms of CH_3SiHCl_2, $Si(CH_3)Cl_3$ and CH_4 in $SiHCl_3$, $SiCl_4$ and recovered hydrogen, respectively, which is consistent with the results of HSC simulation calculations.

Table 5. Detection results of carbon impurities in two types of recovered hydrogen (ppm).

Sample No	Reduction-Recovered Hydrogen				Hydrogenation-Recovered Hydrogen			
	CO	CO_2	CH_4	Methylchlorosilane	CO	CO_2	CH_4	Methylchlorosilane
1	/	/	0.92	/	/	/	371	/
2	/	/	1.17	/	/	/	339	/
3	/	/	0.84	/	/	/	397	/
4	/	/	1.08	/	/	/	381	/
5	/	/	1.08	/	/	/	318	/
6	/	/	0.93	/	/	/	337	/
7	/	/	0.70	/	/	/	341	/
8	/	/	0.95	/	/	/	319	/
9	/	/	0.60	/	/	/	329	/
10	/	/	0.66	/	/	/	329	/

Note: Methylchlorosilanes are mainly composed of CH_3SiHCl_2, $Si(CH_3)Cl_3$, $(CH_3)_3SiCl$, and $(CH_3)_2SiCl_2$.

Combining the results of HSC simulation calculations and detection analysis, the evolution process of carbon impurities during the production of polysilicon via the improved Siemens process is as follows (see Figure 5): a mixture of solid-dissolved carbon atoms and silicon carbide (in metallurgical silicon), $SiH(CH_3)Cl_2$ (in $SiHCl_3$) and $Si(CH_3)Cl_3$ (in $SiCl_4$), solid-dissolved carbon atoms (in polysilicon) and CH_4 (in recycled hydrogen).

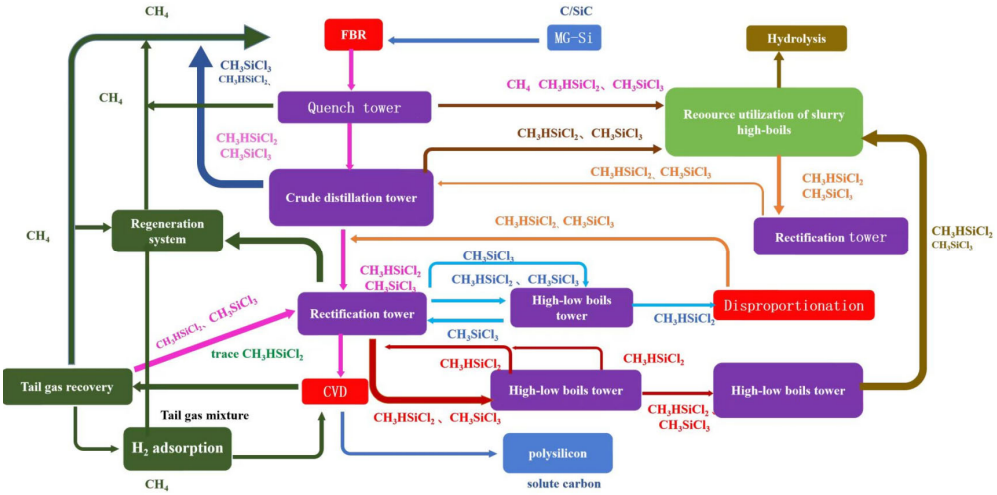


Figure 5. Evolution diagram of carbon impurities in the polysilicon preparation process via the modified Siemens process.

The evolution mechanism of carbon impurities is that the solid-dissolved carbon atoms in metallurgical silicon react with hydrogen to generate CH_4. Subsequently, CH_4 undergoes a cracking reaction synergistically with methylchlorosilane compounds in chlorosilane and CH_4 in recovered hydrogen, yielding $CH_3\cdot$ radicals. The $CH_3\cdot$ radicals combine with Cl· radicals to form chloromethane (CH_3Cl), which then reacts with elemental silicon via the Rochow reaction. Meanwhile, the $CH_3\cdot$ radicals combine with radicals including $SiCl_2\cdot$, $SiCl_3\cdot$, $SiHCl_2\cdot$, SiHCl· and hydrogen radicals (H·), forming a mixture of methylchlorosilanes dominated by $SiH(CH_3)Cl_2$ as well as CH_4. After tail gas separation and distillation purification, $SiH(CH_3)Cl_2$ enters the $SiHCl_3$ stream and is subsequently fed into the reduction process. In the reduction process, it undergoes cracking synergistically with CH_4 in high-purity hydrogen to generate elemental carbon, which deposits in polysilicon in the form of substitutional atoms. Simultaneously, radical rearrangement reactions occur, producing a mixture of methylchlorosilanes dominated by $SiH(CH_3)Cl_2$ along with CH_4, which are then discharged into the tail gas system. Therefore, in the production process of high-purity polysilicon, focus should be placed on developing efficient removal strategies for $SiH(CH_3)Cl_2$ and CH_4 (see Figure 3).

4. Conclusions

Based on HSC simulation calculations and the Gibbs free energy of reactions, this study investigates the existing forms and evolution mechanism of carbon impurities during the polysilicon production via the improved Siemens process. The main conclusions are as follows:

(1) The minimum concentration threshold for the formation of silicon carbide (SiC) compounds in the silicon melt (65 ppm) is higher than the carbon impurity concentration in polysilicon but lower than that in metallurgical silicon. The main existing form of carbon impurities in metallurgical silicon is a mixture of solute carbon atoms and SiC. In contrast, carbon impurities in high-purity polysilicon mainly exist in the form of solute atoms.

(2) In the direct synthesis and cold hydrogenation processes, the main potential existing forms of carbon impurities are $SiH(CH_3)Cl_2$ and CH_4, accompanied by the by-production of $Si(CH_3)_3Cl$ and $Si(CH_3)Cl_3$. Through distillation purification, redistribution and enrichment of methylchlorosilanes occur among different components. Among these components, the carbon impurities in refined $SiHCl_3$ are mainly present in the form of $SiH(CH_3)Cl_2$.

(3) In the reduction system, the main existing forms associated with carbon impurities are substitutional carbon atoms, CH_4 and $SiH(CH_3)Cl_2$, accompanied by a small amount of $Si(CH_3)_3Cl$. These substances enter the tail gas recovery system, and after gas–liquid separation, CH_4 accounts for the main component in the recovered hydrogen.

(4) In the production process of polysilicon via the improved Siemens method, the evolution process of carbon impurities is as follows: a mixture of solid-dissolved carbon atoms and silicon carbide (metallurgical silicon), $SiH(CH_3)Cl_2$ (in $SiHCl_3$) and $Si(CH_3)Cl_3$ (in $SiCl_4$), solid-dissolved carbon atoms (in polysilicon) and methane (in recycled hydrogen). This process is basically consistent with the sampling and testing results of different working procedures.

Author Contributions: Conceived the central idea, Y.H. and G.H.; investigation, Y.H. and X.L.; performed research and analyzed data, Y.H. and X.L.; writing—original draft preparation, Y.H.; writing—draft discussion, Y.H. and X.L.; writing—review and editing, Y.H., X.L. and G.H.; supervision, G.H.; project administration, G.H.; funding acquisition, X.L. and G.H. All authors have read and agreed to the published version of the manuscript.

Funding: This research was funded by the Key Research and Development Program of the Xinjiang Uygur Autonomous Region (Grant no. 2023B01004).

Institutional Review Board Statement: Not applicable.

Informed Consent Statement: Informed consent was obtained from all subjects involved in the study.

Data Availability Statement: The original contributions presented in this study are included in the article. Further inquiries can be directed to the corresponding author.

Conflicts of Interest: The authors declare no conflicts of interest. Authors Yu Hou and Xueqian Lv were employed by the company Xinjiang Xinte Crystalline Silicon High-Tech Co., Ltd. The remaining authors declare that the research was conducted in the absence of any commercial or financial relationships that could be construed as a potential conflict of interest.

References

1. Yang, D.R. *Materials for Solar Cells*; Chemical Industry Press: Beijing, China, 2018.
2. Han, Z.S. *Semiconductor Manufacturing Technology*; Publishing House of Electronics Industry: Beijing, China, 2015.
3. O'Mara, W.C.; Herring, R.B.; Hunt, L.P. *Handbook of Semiconductor Silicon Technology*; Noyes Publications: New York, NY, USA, 1990.
4. Zhou, J.Z.; Zhan, B.; Lv, B.; Guo, Y.; Jiang, B. Contribution Rates and Simulation Model Refinement for Polysilicon Films Deposited by Large-Sized Tubular Low-Pressure Chemical Vapor Deposition Reactors. *Materials* **2024**, *17*, 5952. [CrossRef] [PubMed]

5. Que, D.L. *Silicon Materials Science and Technology*; Zhejiang University Press: Hangzhou, China, 2000.
6. Yuan, X.P.; Guo, L.J.; Lv, Q.H.; Zhao, D.; Liao, H.; Ma, W.H.; Hou, Y.Q.; Shen, J.L. Product quality research in the industrialized preparation of electronic grade polysilicon: A review of impurity sources and control strategies. *Renew. Sustain. Energy Rev.* **2025**, *214*, 115569. [CrossRef]
7. Cao, L.L.; Cai, Y.G.; Zong, B.; Wei, D.L. Influencing factors and control measures of carbon content in polysilicon products. *Mod. Chem. Ind.* **2019**, *39*, 183–186.
8. Chen, Y.M.; Weng, B.F.; Liu, Y.N. Analyses of Polychlorosilanes and Methylchlorosilanes Containing in Synthesized Trichlorosilane. *Chem. Newsl.* **2014**, *77*, 274–277.
9. Yang, H. Study on gas chromatography-mass spectrometry method for determination of 4 kind of methylchlorosilane in high purity trichlorosilane. *Anal. Instrum.* **2019**, *1*, 88–92.
10. Lewis, K.M.; Rethwisch, D.G. *Catalyzed Direct Reactions of Silicon*; Elsevier: New York, NY, USA, 1993.
11. Coleman, L.; Buffasultant, E.C. Optimize Your Chlorosilane Distillation Columns. In *Proceedings of the Silicon For the Chemical and Solar Industry XIII, Kristiansand, Norway, 13–16 June 2016*; Norwegian University of Science and Technology: Trondheim, Norway, 2016.
12. Vaisarová, V.; Bažant, V.; Chvalovský, V. Organosilicon compounds. LV. Dipole moments of substituted allylsilanes and benzylsilanes. *Collect. Czechoslov. Chem. Commun.* **1968**, *33*, 850–858. [CrossRef]
13. Lai, G.Q.; Xin, S.M. *Youjigui Chanpin Hecheng Gongyi Ji Yingyong*; Chemical Industry Press: Beijing, China, 2009.
14. Yang, D.; Wang, F.; Wan, Y. Research progress on separation process of methyl dichlorosilane from trichlorsilane. *Inorg. Chem. Ind.* **2021**, *53*, 30–34.
15. Lepage, J.L.; Soula, G. Preparation of Silane from Methyldichlorosi-Lane and Chlorosilanes. U.S. Patent 4605543, 12 August 1986.
16. Tanaka, S. Method for Producing Trichlorosilane. WO Patent 2011111335A, 15 September 2011.
17. Atkins, P.W.; Paula, J.D. *Physical Chemistry*; Oxford University Press: New York, NY, USA; Oxford, UK, 2006.
18. Zou, B.S.; Jiang, Y.F.; Liao, G.A.; Shen, Y.Q.; Wang, X.P.; Wang, N.; Wang, Y.; He, C.; Gao, F. Preparation of Al-Ti-Sc master alloys and refining effects on the 6016 aluminum alloy. *J. Alloys Compd.* **2024**, *985*, 174094. [CrossRef]
19. *GB_T 14849.6-2014*; Methods for Chemical Analysis of Silicon Metal. Part 6: Determination of Carbon. Infrared Absorption Method. Standardization Administration of the People's Republic of China: Beijing, China, 2014.
20. *YS/T 1300-2019*; Determination of Methyldichlorosilane, Trimethylchlorosilane and Methyltrichlorosilane in Chlorosilanes-Gas Chromatography-Mass Spectrometry Method. Ministry of Industry and Information Technology of the People's Republic of China: Beijing, China, 2019.
21. *GB/T 3634.2-2011*; Hydrogen—Part 2: Pure Hydrogen, High Pure Hydrogen and Ultra-Pure Hydrogen. Standardization Administration of the People's Republic of China: Beijing, China, 2011.
22. Gu, Y.J.; Gong, S.K. *Analysis and Testing Technology on Materials*; Central South University Press: Changsha, China, 2011.
23. *GB/T 29057-2023*; Practice for Evaluation of Polocrystalline Silicon Rods by Float-Zone Crystal Growth and Spectroscopy. Standardization Administration of the People's Republic of China: Beijing, China, 2023.
24. *GB/T 35306-2023*; Determination of Carbon and Oxygen Content in Silicon Single Crystal Low Temperature Fourier Transform Infrared Spectroscopy. Standardization Administration of the People's Republic of China: Beijing, China, 2023.
25. Dalaker, H.; Tangstad, M. Time and Temperature Dependence of the Solubility of Carbon in Liquid Silicon Equilibrated with Silicon Carbide and Its Dependence on Boron Levels. *Mater. Trans.* **2009**, *50*, 1152–1156. [CrossRef]
26. Tan, Y.; Qin, S.Q.; Shi, S.; Jiang, D.C. Research Progress on Light Elements (C, N, O) in Solar-grade Silicon. *J. Mater. Eng.* **2017**, *45*, 112–118.
27. Svanem, J.P.; Røe, T. Analytical Method to Measure Different Forms of Carbon in Silicon. In *Proceedings of the Silicon For the Chemical and Solar Industry XI, Bergen-Ulvik, Norway, 25–29 June 2012*; Norwegian University of Science and Technology: Trondheim, Norway, 2012.
28. Ding, W.J. Mechanism and Kinetic Studies of a Two-Step Reactions Process for Metallurgical Slicon to Silane. Ph.D. Thesis, Shanghai Jiao Tong Unversity, Shanghai, China, March 2015.
29. Xing, Q.Y.; Xu, R.Q.; Zhou, Z.; Pei, W.W. *Basic Organic Chemistry*; Higher Education Press: Beijing, China, 1993.
30. Chernyavsky, L.I.; Titov, V.A.; Sysoev, S.V. Thermodynamic Simulation of Silicon Deposition from the Gas Phase of Si-Cl-H System. *Inoorganic Mater.* **2009**, *45*, 517–521. [CrossRef]
31. Jong, F.d.; Meyyappan, M. Numerical siulation of silicon carbide chemicai vapor deposition. *Diam. Relat. Mater.* **1996**, *5*, 141–150. [CrossRef]

Disclaimer/Publisher's Note: The statements, opinions and data contained in all publications are solely those of the individual author(s) and contributor(s) and not of MDPI and/or the editor(s). MDPI and/or the editor(s) disclaim responsibility for any injury to people or property resulting from any ideas, methods, instructions or products referred to in the content.